

# In-vitro – In-vivo Characterization of Glimepiride Lipid Nanoparticulates Prepared by Combined Approach of Precipitation and Complexation

Sajeev Kumar B\* and Divakar Goli

Department of Pharmaceutics, Faculty of Pharmacy, Acharya & BM Reddy College of Pharmacy, Soldevanahalli, Bengaluru 560 017, India.

(\* ) Corresponding author: Email sajeevkumarb@acharya.ac.in  
(Received: 13 November 2018 and Accepted: 09 December 2018)

## Abstract

Novel lipid nanoparticulates (NCs) were developed by a combined approach of precipitation and complexation with an aim to improve the solubility, stability and targeting efficiency of glimepiride (GLP). GLP NCs were prepared by precipitation process using PEG 20000 and further complexed with phospholipon90G (P90G). The NCs were evaluated for physicochemical characterization, such as drug loading, saturation solubility (SS) and particle characterization studies. The solid state characterization studies were performed using X-ray powder diffractometry (XRPD), differential scanning calorimetry (DSC), infrared spectroscopy (FTIR) and scanning electron microscopy (SEM). Further in-vitro dissolution studies and in vivo (drug targeting) studies were also performed. Short term (3 months) stability studies were conducted on most satisfactory NCs. GLP P90G NCs exhibited three folds increase in saturation solubility. Particle size of NCs was ranging from between 210-240 nm. The dissolution and in vitro stability of NCs were superior compared to pure GLP. XRPD and DSC analysis proved that crystallinity prevailed in NCs, but with a slight change in crystal structure. SEM analysis indicated spherical shaped particles with a lipid coat. The NCs were found to be stable during the period of study. In vivo studies on optimized NCs showed slightly higher drug concentration (1.38 µg/ml) in pancreas of rat than that of pure GLP. It can be concluded that solubility and stability of GLPNCs were significantly improved by P90G complexation. Also, P90G (phospholipids) could be effectively used in enhancing the targeting efficiency and pharmacokinetics of glimepiride.

**Keywords:** Nanoparticles, Nanonization, Phospholipids, Pancreatic targeting, Surface properties.

## 1. INTRODUCTION

Diabetes mellitus is a disease which has become an epidemic in the world. Based on the data from 40 countries around the world, published by WHO, it is estimated that by 2030, the number of people suffering from diabetes may rise to 366 million [1]. Type II diabetes otherwise known as non-insulin-dependent diabetes mellitus (NIDDM) is a chronic metabolic disorder that results from defects in both insulin action and secretion [2]. Controlling glycemia is an important part of preventing serious complications of

diabetes. The development of new classes of blood glucose-lowering medications to supplement the older therapies, such as lifestyle-directed interventions, insulin, sulfonylureas, and metformin, has increased the number of treatment options available for type 2 diabetes [3].

Treatment of diabetes involves wide use of insulin. Insulin therapy offer draw backs like discomfort, inconvenience of multiple injections, hyperinsulinemia, pain, itching, allergy and insulin dystrophy after repetitive

dosing. Regular utilization of such medications can drive the overall health care cost in patients. An alternative to insulin injections are administration of conventional oral hypoglycemic agents. Interestingly, oral delivery of products has much recognition and oral delivery of biopharmaceuticals is highly desirable as it provides ease of administration and improves patient compliance. But oral administration still remains as an elusive goal in drug delivery. Administration of oral hypoglycemic agents has serious limitations and includes short duration of action, non uniqueness in dosage regimen and non customized plasma profiles and patient incompliance [4].

The major obstacles in oral delivery of drugs include issues concerned with poor solubility and bioavailability, protein instability, degradation, poor gastrointestinal (GI) permeability, presence of various chemical and enzymatic barriers in GI tract [5]. Various absorption enhancing technologies have been applied by many pharmaceuticals to address the problem but their success remains partial. Conversely, challenges remain ahead owing to the limitations on the size of the macromolecules that can be delivered. As majority of the dosage regimen is towards oral dosage forms, feedback from industry surveys shows bioavailability and solubility issues as top technical concerns in drug development [6].

To improve the dissolution and bioavailability of sparingly soluble drugs, researchers have employed various techniques such as particle engineering, salt selection and amorphization of the compound, use of surface-active agents or cosolvents, polymeric stabilizers, and solid dispersions and solutions [7]. In addition to the above, some physical modifications techniques include micronization and sonocrystallization to improve solubility [8]. Recently nanonization have emerged as a

promising technique to improve the solubility and bioavailability of drugs. This technique progresses beyond micronization to further reduce the particle size below 1  $\mu\text{m}$ . This strategy increases the surface area-to volume ratios of powders, changes the crystalline structure of drug (s) and develops nanomaterials suitable for drug delivery [9, 10].

The above nonconventional and physical methods to improve solubility and bioavailability of a drug have their own limits as the particles are not engineered to the current requirement of the therapy. The designed particles regularly undergo enzymatic and chemical actions resulting in degradation thus decreasing bioavailability [11]. This highlights the importance of creating new possibilities for development of smart engineered particles (novel drug delivery systems) for drug therapy and delivery as it may possibly withstand the chemical and enzymatic actions. Consequently novel drug delivery systems can overcome the limitations of conventional dosage forms like decreased bioavailability and targetability, higher and frequent dosing and variable plasma levels.

Novel drug delivery systems include solid lipid nanoparticles, nanocrystals, nanosuspensions, carbon nanotubes, nanoshells, polymeric micelles, quantum dots, dendrimers and fullerenes [12]. Processes involved in the preparation of nanoparticles include top down, bottom up, combined approach and spray drying. Top down involves milling and high pressure homogenization (HPH), while bottom up include nanoprecipitation using polymers. The above processes increase the saturation solubility and dissolution velocity. A drawback in HPH and milling is that it attracts more residues from excipients causing instability and toxicity [13].

The major limitations observed in nanoformulations are the instability of

particles both *in vitro* and *in vivo*. These nanoparticles undergo excessive particle aggregation and crystal growth on contact with fluids or electrolytes. This results in nanoparticles to lose their surface and functional properties [14, 15]. The limitations could be resolved by incorporating nanoparticles in carriers or by attaching ligands, or else by increasing its stealthiness using lipids [16]. This not only improves *in vivo* stability but also provides a more complete and consistent absorption profile of the drug similar to that of solid lipid nanoparticles (SLN) [17, 18].

Development of LNPs of antidiabetic drugs to improve bioavailability and targetability of drug to pancreatic cell to secrete insulin study is limited. Majority of the works have been focused towards solubility enhancement by developing them as solid dispersions of drugs, salt formation of ionizable drugs, complexing with cyclodextrins, and conjugation to dendrimers [19]. Studies on solid micro and nanoparticles, and solid dispersions of glibenclamide, glimepiride and metformin have shown similar results with less of drug targeting due to poor surface properties, variable plasma level and unreliable therapeutic response or greater incidence of side effects [20]. Perhaps the reason for poor *in vivo* performance is due to the lack of functionalized particles that might offer superior surface properties (high *in vivo* stability and *in vivo* performance).

Development of functionalized NPs uses principles and techniques of nanonization and optimization restricting the size of the particle within a nano range so as to improve the affinity and permeability towards cells. They consist of ligands and groups to target receptors, enzymes, peptides, proteins and antibodies. These NPs can withstand the *in vivo* conditions and protect the drug core [21].

At present, development of novel drug delivery systems (nanodevices) for diabetes is highly essential. This could facilitate ease of administration, improve patient compliance and offer better blood glucose management [22]. Lately, targeted drug nanocarriers (TDNPs) are widely explored for diabetes therapy. TDNPs can carry poorly soluble, unstable or systemically toxic drugs with extended blood half-lives [23]. The presence of targeting molecules at the surface of nanocarriers can increase its targeting ability resulting in higher drug accumulation. This prevents degradation or inactivation of drug during transit and protects the body from adverse reactions because of inappropriate disposition [24]. Existing novel drug delivery systems possess major limitations like stability of particles, high interactions with blood components, high clearance rate due to small size, MPS uptake, difficulty in membrane crossing, increased chemical reactivity and toxicity, and nonspecific targeting and drug accumulation [25].

In the present study novel lipid nanoparticulates (nanocrystals) of glimepiride (GLP) was developed by precipitation process and complexed using lipids. Glimepiride (GLP) is as a weakly acidic, once-daily, oral hypoglycemic agent belonging to BCS Class II. BCS is based on a scientific framework describing the three rate limiting steps in oral absorption. The three necessary steps for a drug to be absorbed are (1) release of drug from dosage forms, (2) maintenance of dissolved state throughout gastrointestinal (GI) track, and (3) permeation of drug molecules through GI membrane into hepatic circulation [26]. Glimepiride shows low pH dependent solubility. In acidic and neutral aqueous media, glimepiride exhibits very poor solubility at 37<sup>0</sup> C (<0.004 mg/ml). In media pH>7, solubility of drug is slightly increased to 0.02 mg/ml. These poorly water soluble

drugs provide challenges to deliver them in an active and absorbable form to the desired absorption site using physiologically safe excipients. GLP also has lower binding affinity for the beta cell receptor, a two to three folds faster rate of association at the receptor site and an eight to nine folds faster rate of disassociation [27]. GLP, with log *P* value of 3.2, p*K*<sub>a</sub> of 6.2 and a low oral dose (1-4 mg), has a strong rationale as a good candidate to be developed into nanocrystals [28].

Development of functionalized nanoparticulates could be a new way to overcome the obstacles of diabetes therapy. Accordingly, functionalized nanocrystals of glimepiride could offer enhanced surface properties that can permeate, target a specific site, initiate better biodistribution and blood circulation, reduced drug clearance and MPS uptake. This facilitates improved bioavailability, regulates blood glucose effectively and may probably help in reducing frequent dosing and dose size.

The objective of the study was to formulate GLP NCs by precipitation technique to improve aqueous solubility and complex GLP NCs with phospholipids (P90G) to improve stability and drug targeting efficacy. The LNCs were evaluated for various physicochemical characterization, stability analysis and *in-vivo* performance studies.

## 2. MATERIALS AND METHODS

### 2.1 Materials

Glimepiride sample was obtained from S.D Biomed labs (Malaysia). PEG 20000 and Phospholipon<sup>®</sup> (P90G) were procured from Sigma Aldrich, Malaysia and GmbH, Germany. Tween<sup>®</sup> 80, sodium dodecyl sulfate, polysorbate 80, dichloromethane and methanol were purchased from R and M Chemicals, Malaysia. Deionized water was obtained from Millipore, MilliQ-Plus. All

the other solvents and reagents used were of AR grade.

### 2.1.1 Preparation of Glimepiride-Polyethylene Glycol Nano Crystals (GLP-PEG NCs)

Glimepiride PEG NC's were prepared by precipitation technique. GLP was dissolved in 10 ml of dichloromethane (DCM). PEG 20000 was added to the drug solution and stirred using a magnetic stirrer (Erla-EMS H 7000) at a temperature not exceeding 61°C for a period of 20 min. The drug-polymeric solution was injected slowly (1ml/min) into an aqueous phase containing a surfactant (Tween 80 - 2.5% w/v). Stirring was continued for 4 h at 450 rpm to precipitate the NCs. The volume of dispersion (80 ml) was adjusted to 100 ml using double distilled water and further stirred for 4 h at room temperature. Later, the solution was gently heated (65°C) with magnetic stirring (Erla- EMS H7000, Korea) for 45 min to remove the organic solvent. The contents were centrifuged (Heraeus - Labofuge 200, Germany) at 5000 rpm for 15 min to separate the NCs. The clear supernatant liquid was discarded; the thick viscous dispersion was collected and further redispersed in 15 ml of distilled water and recentrifuged (Hitachi - CT15E, Taiwan) at 20000 rpm for 10 min [29, 30]. The precipitated NCs were recovered using a vacuum filter (Kontes-Ultraware-USA, 0.2 µm,) and dried in a hot air oven (Mettler - UF110, Germany) at 35°C for 20 min. Formulations were prepared with different GLP:PEG ratios (1:1, 1:2, 1:4, 1:8 and 2:1 and were coded as F1, F2, F3, F4 and F5 respectively.

### 2.1.2 Complexation of GLP-PEG NCs with Phospholipon (P90G)

All batches (F1, F2, F3, F4 and F5) were subjected to complexation using P90G. From each batch, 50 mg of dried NCs

(quantity equivalent to 4 mg drug) were accurately weighed and dispersed in 50 ml of phosphate buffer (pH 7.8) containing 0.1% w/v of Tween 80, by gentle stirring (Erla- EMS H7000, Korea) for 15 min. P90G (2% w/v) previously solubilized in chloroform was gradually added (2 ml/min) to the dispersion and stirred using a magnetic stirrer (Erla- EMS H7000, Korea) at 250 rpm for 40 min. During stirring, the temperature was maintained below 60°C (melting point of P90G). Further, the dispersion was transferred to a shaking incubator (Daiki Scientific - DK-SI 010, Korea) and shaken at 120 rpm for 1 h at 15°C. Mannitol (5% w/v) as cryoprotectant was added to the dispersion and shaking was continued for 15 min prior to lyophilization [31, 32]. The formulations F1, F2, F3, F4 and F5, complexed with phospholipon (P90G) were coded as F1P, F2P, F3P, F4P and F5P respectively.

### 2.1.3 Freeze Drying

The milky homogenous dispersion (F1P, F2P, F3P, F4P and F5P NCs) was subjected to freeze drying in a freeze dryer (Thermo scientific, USA), with an inbuilt Pirani 501 microprocessor. The samples were lyophilized at a slow freezing temperature (shelf temperature -40°C at 6 torr and 10<sup>-1</sup> mbar pressure) for 11 h. The lyophilized products were stored in borosilicate glass vials and stored in a dessicator, at room temperature, until further use.

## 3. PHYSICOCHEMICAL CHARACTERIZATION

### 3.1 Drug Loading (DL) and Process Yield (PY)

Drug loading and process yield for all the complexed formulations viz., F1P, F2P, F3P, F4P and F5P was carried out using the following procedure. 50 mg of NCs were accurately weighed and dissolved in 10 ml of methanol and vortexed for 5 min in a tube

mixer (VTX 3000 L, LMS, China). The solution was filtered using a disc filter (0.45 µm, Titan 2 Nylon, USA) and the absorbance was measured at 223 nm, against a similarly treated blank. The measurements were carried out using UV-Visible spectrophotometer (Beckman coulter- DU 800, USA). The procedure was repeated in triplicate for all samples (n=3). The percentage drug loading and process yield were calculated from equation 1 and 2 respectively [33].

$$\% \text{ DL} = [\text{Amount of drug loaded in NCs} / \text{amount of drug added} + \text{amount of excipients added}] \times 100 \quad (1)$$

$$\text{Process yield} = \frac{\text{Practical yield}}{\text{Theoretical yield}} \times 100 \quad (2)$$

### 3.2 Saturation Solubility (SS)

1 g of freeze dried NC was added to 10 ml of distilled water and stirred at 125 rpm, in an orbital shaker (Erla - ES 203D, Korea) for 24 h, at room temperature to ensure saturation. The contents were filtered using a disc filter (0.45 µm, Titan 2 Nylon, USA) and diluted suitably using phosphate buffer (pH 7.8). The samples were analyzed in a UV-Visible spectrophotometer (Beckman coulter- DU 800, USA) at 223 nm against a blank. The procedure was carried out in triplicate, for all the complexed formulations viz., F1P, F2P, F3P, F4P and F5P. The saturation solubility was calculated and expressed as µg/5ml [34].

Saturation solubility can be explained by Kelvin and the Ostwald-Freundlich equation.

$$RT/V_m \ln = S/S_0 = 2\gamma/r \quad (3)$$

Where,  $S$  is the solubility of small particles of size ' $r$ ',  $S_0$  is the equilibrium solubility,  $R$  is universal gas constant,  $T$  is the temperature,  $\gamma$  is surface tension and  $V_m$  is

molar volume. Equation 3 is an extension of Kelvin equation which is given as,

$$\rho V RT/M \ln S_r/S_\infty = 2 \lambda_{sl}/r \quad (4)$$

The saturation solubility is given as,

$$S = S_\infty \exp(2\gamma M/r\rho RT) \quad (5)$$

where,  $S$  is the saturation solubility of nanonized drug,  $S_\infty$  is the saturation solubility of an infinitely large drug crystal,  $\gamma$  is the crystal medium interfacial tension,  $M$  is the compound molecular weight,  $r$  is the particle radius,  $\rho$  is the density,  $R$  is universal gas constant, and  $T$  is the temperature (Muller and Peters; 1998). The percentage solubility was calculated using equation 6.

$$\text{Solubility} = \text{mass of NC/mass of water} \times 100 \quad (6)$$

### 3.3 Optical Clarity (OC)

Optical clarity for all the complexed formulations viz., F1P, F2P, F3P, F4P and F5P was determined by the following procedure. An amount of NC equivalent to 4 mg of GLP was dispersed in 100 ml of phosphate buffer (pH 7.8) and mixed well in a measuring cylinder. 5 ml of sample was withdrawn at periodic intervals (0 to 240 min) and suitably diluted using 0.1N NaOH, further filtered using a disc filter (0.45  $\mu\text{m}$ , Titan 2 Nylon, USA). The optical clarity was determined by measuring the absorbances of samples in a UV-Visible spectrophotometer (Beckman coulter-DU 800, USA) at 223 nm against a blank. The procedure was carried out in triplicate [35].

### 3.4 Particle Characterization

#### 3.4.1 Photon Correlation Spectroscopy (PCS)

The mean particle size and polydispersity index (PDI) of pure GLP, GLP-PEG NC's

and complexed GLP-PEG NCs were measured using Malvern Zetasizer Nano ZS (Malvern Instruments, UK). 2 mg of sample was dispersed in 150 ml of deionized water containing 0.5% w/v of sodium dodecyl sulfate (SDS). The dispersion was sonicated in a bath sonicator (Power sonic 410, Lab Tech, Korea) and left aside for 24 h prior to analysis. 5  $\mu\text{l}$  of suspension was diluted with 2 ml of deionized water and the samples were pipetted into disposable polystyrene cuvettes. Samples were analyzed to determine the mean particle size and polydispersity index, at fixed angle of  $90^\circ$  at  $25^\circ\text{C}$ , after five runs. A refractive index of 1.30 was used for the dispersant [36,37]. Each measurement was performed in triplicate.

#### 3.4.2 Zeta Potential Measurement (ZP)

The zeta potential of pure GLP, precipitated GLP-PEG NC's and complexed GLP-PEG NCs were measured using Malvern Zetasizer Nano ZS (M3-PALS, Malvern Instruments, UK). Samples were dispersed in deionized water and left for 24 h and later, injected into a clear disposable zeta cell after suitable dilution with deionized water. Air bubbles if any, in the zeta cells, were removed by tapping. The samples were measured for average zeta potential (mV) after 3 consecutive scans.

## 4. SOLID STATE CHARACTERIZATION

### 4.1 X-Ray Powder Diffraction (XRPD)

XRPD diffractograms of pure GLP, PEG 20000, physical mixtures (GLP:PEG-1:1) and complexed GLP-PEG NCs were recorded in X-ray diffractometer (Bruker AXS D8, Germany) with Anton Paar, TTK 450 temperature attachment, using Si (Li) PSD detector. The samples were placed in a glass sample holder and Cu ka radiation was generated at 30 mA and 40 Kv. The samples

were scanned from 3° to 80° with a step size of 0.02° in duplicate.

#### 4.2 Differential Scanning Calorimetry (DSC)

DSC analysis of pure GLP, PEG 20000, physical mixture of drug and polymer (1:1) and complexed GLP-PEG NCs were analyzed in a DSC calorimeter (TA Instruments, Q200, USA), equipped with a liquid nitrogen cooling system. About 5 mg of sample was loaded into an open aluminum pan, crimped, sealed and further examined at a scanning rate of 10°C/min from 15 to 200°C under nitrogen atmosphere (flow rate 100 ml/min) at room temperature. High purity indium was used to calibrate the heat flow and heat capacity of the instruments. The analysis was performed in duplicate.

#### 4.3 FTIR Analysis

Spectra of pure GLP, PEG 20000, physical mixture (GLP: PEG-1:1) and complexed GLP-PEG NCs were recorded in FT-IR spectrophotometer (Thermo Nicolet, Avatar 370, USA). 2 mg of sample was mixed with 1% KBr, compressed into a pellet and scanned for 4 seconds at a resolution of 4 cm<sup>-1</sup> from 4000 to 400 cm<sup>-1</sup>.

#### 4.4 Scanning Electron Microscopy Analysis (SEM)

Morphological evaluation of NCs was performed using a scanning electron microscope (LEO 1530, Gemini, Germany). The samples were mounted to steel stubs (Jeol - 10 mm Dia x 5 mm) using a double sided adhesive tape and sputtered with a thin layer of Au at 20 mA, under 1x10<sup>-1</sup> bar vacuum for 10 min using a sputter coater (EM S550X - Electron microscopy sciences) and was operated at an acceleration voltage of 3 kV. SEM images of pure GLP, F1 NCs, F1P NCs, F1P NCs dispersed in water and

air dried, and F1 NCs in aggregated form before complexation were recorded.

### 5. IN VITRO DISSOLUTION STUDIES

Dissolution studies from pure GLP and complexed GLP-PEG NCs were performed using a USP XXIII, 8-station rotating paddle apparatus (Electrolab-TDT 067, India) with a speed of 75 rpm (±1) and at a temperature of 37 ± 0.5°C. 900 ml of phosphate buffer (pH 7.8) was used as the dissolution medium. An amount of NC equivalent to 4 mg was added to the dissolution media. 5 ml of sample was withdrawn at periodic intervals (0 to 240 min) and suitably diluted using 0.1N NaOH, further filtered using a disc filter (0.45 µm, Titan 2 Nylon, USA). The absorbances were measured against a blank, in a UV-Visible spectrophotometer (Beckman coulter, DU-800, USA) at 223 nm. Sink conditions were maintained throughout the studies. The content of GLP was calculated from the standard curve [OD = 0.0488 x concentration + 0.0109 (r<sup>2</sup> = 0.999) [38]. The procedure was carried out in triplicate. The cumulative percentage of GLP released was plotted against the time intervals to obtain the dissolution profile.

#### 5.1 Quantity of Drug Release (Q<sub>min</sub>) and Dissolution Data Treatment (% DE and MDT)

The quantity of drug released at 5, 10, 30 and 60 min (Q<sub>05</sub>, Q<sub>10</sub>, Q<sub>30</sub> and Q<sub>60</sub>) and dissolution parameters such as percentage dissolution efficiency (% DE) and mean dissolution time (MDT) were used to further characterize the drug release profiles. DE, defined as the area under the dissolution curve up to a certain time “t”, is expressed as percentage of the area of the rectangle arising from 100% dissolution in the same time. The % DE and MDT were calculated from the equation given below [39, 40].

$$\% DE = \left( \frac{\int_0^t y \cdot dt}{y_{100} \cdot t} \right) 100 \quad (7)$$

$$\text{MDT} = \frac{\sum_{j=1}^n t_j \Delta M_j}{\sum_{j=1}^n \Delta M_j} \quad (8)$$

Where  $j$  is the sample number,  $n$  is the number of dissolution sample times,  $t_j$  is the time at midpoint between  $t_j$  and  $t_{j-1}$  (calculated with the expression  $(t_j + t_{j-1})/2$ ) and  $\Delta M_j$  is the additional amount of drug dissolved between  $t_j$  and  $t_{j-1}$ .

## 6. IN VIVO STUDIES

The animal experiment was evaluated and approved by the Committee for the Purpose of Supervision and Control of Experiments on Animals, India (1410/C11/CPCSEA). The *in vivo* studies were performed on most satisfactory formulation F1P, in order to evaluate the effectiveness of drug distribution to pancreas. Healthy, male, adult, Wistar rat's weighing 180-220 g, were housed in well ventilated rooms in a large cage for 12 h light/12 h dark cycle throughout the experimental period. The animals were provided with food and water ad libitum. The animals were divided into three groups, each group consisting of 3 rats. Group 1 received the pure GLP, Group 2 received the complexed GLP-PEG NCs (F1P) and Group 3, which received GLP-PEG NCs (F1), was the control group.

Pure GLP, test formulation (F1P) and precipitated NCs (F1) were administered orally as suspension (samples dispersed in 2 ml of distilled water) to male Wistar rats, using oral gavage, at a dose of 10 mg/kg. Rats were sacrificed following deep anesthesia and by abdominal incision pancreas was removed, 1 h post administration. Pancreas was washed with saline and weighed accurately. Tissue homogenate was prepared with PBS. The homogenate was centrifuged at 3500 rpm (Hitachi - CT15E, Taiwan) for 20 min.

Supernatant collected was stored at  $-20^{\circ}\text{C}$  until analysis.

### 6.1 Extraction and Deproteinization of Sample

The amount of drug reaching the pancreas was quantitatively estimated using HPLC (LC-2010HT, Shimadzu, Japan). 1 ml of tissue homogenate was mixed with 2 ml of acetonitrile and allowed to stand for 5 min. The content was centrifuged (Hitachi - CT15E, Taiwan) at 5000 rpm for 10 min and the clear supernatant was collected and stored at  $4^{\circ}\text{C}$ . The chromatographic system consisted of C18 Bonda Pack ( $5\ \mu\text{m}$ ,  $150 \times 4.6\text{mm D}$ ) column as the stationary phase and 0.1% orthophosphoric acid, acetonitrile, methanol (20:50:30) as the mobile phase. The flow rate of mobile phase was 1ml/min and 20  $\mu\text{l}$  of supernatant was injected. The analyte was detected at 210 nm. The retention time (RT) and peak area (AUC) were recorded. The amount of drug reaching the pancreas (drug concentration) was determined from the slope  $Y = 21385 \pm 1437$  ( $r^2 = 0.999$ ).

## 7. STATISTICAL ANALYSIS

Statistics, using one-way analysis of variance (ANOVA) was performed in order to demonstrate differences (ANOVA) between *in vitro* and *in vivo* release studies. A post hoc Bonferroni test was applied to establish the statistically significant difference between the subgroups. Student's t test was also applied to compare means between two groups for expressing the significance. Differences were considered to be significant at a level of  $p < 0.05$ .

## 8. SHORT TERM STABILITY STUDIES

Short term stability studies were carried out for the most satisfactory formulation F1P. Formulation was placed in clean airtight glass vials and stored at different temperature conditions (room temperature

and 40°C/75% RH) over a period of 3 months. During the period, the samples were evaluated for drug content, average particle size and observed for any shift in FT-IR spectra.

## 9. RESULTS

### 9.1 Drug Loading, Process Yield and Saturation Solubility

**Table 1.** Drug loading, process yield and solubility data of complexed GLP-PEG NCs.

| Batch    | Drug loading* (%) | Process yield* (%) | Saturation solubility* (µg/5 ml) | Percentage solubility* (mg/100 ml) |
|----------|-------------------|--------------------|----------------------------------|------------------------------------|
| Pure GLP | -                 | -                  | 0.059 ± 0.1                      | 7.41 ± 2.02                        |
| F1P      | 42.30 ± 1.65      | 82.20 ± 3.30       | 0.159 ± 0.02                     | 21.68 ± 1.31                       |
| F2P      | 58.11 ± 1.53      | 78.46 ± 7.34       | 0.194 ± 0.04                     | 19.43 ± 1.28                       |
| F3P      | 82.89 ± 3.07      | 74.36 ± 8.98       | 0.109 ± 0.02                     | 14.57 ± 2.35                       |
| F4P      | 91.73 ± 2.47      | 80.11 ± 4.73       | 0.108 ± 0.05                     | 14.79 ± 1.81                       |
| F5P      | 21.17 ± 2.54      | 72.24 ± 4.77       | 0.111 ± 0.04                     | 15.96 ± 0.35                       |

(\*) Average of three determinations, ± SD

### 9.2 Optical Clarity

Optical clarity measurements were performed using, UV-Visible spectrophotometer. This measures the amount of light of a given wave length transmitted by the solution. A graph was plotted (absorbance vs time (min)) to analyze the clarity. The absorbance values of complexed NCs after solubilization in 100 ml phosphate buffer (pH 7.8) are depicted in Fig.1. The optical clarity being rated as F1P > F5P > F3P > F2P > F4P. The clarity was found to increase for batches F1P and F5P. Formulation F2P and F4P were cloudier due to large crystalline particles. These exhibited higher absorbance values compared to other samples as a result of higher scattering of incidental light. Optical clarity results of F1P and F5P shows the NCs were dispersed as fine powder in the medium.

### 9.3 Particle Size Analysis

The particle size analysis for pure GLP, precipitated and complexed NCs are shown

As presented in Table 1, the percentage drug loaded was ranging from 21.17 to 91.70 for the complexed formulations. The process yield was between 72.24 to 82.20 %. The saturation solubility was found to increase by three folds for all complexed formulations as compared to pure GLP.

in Table 2. The average particle size of pure GLP was 2066 nm, while that of precipitated NCs was in the range of 30-1920 nm.

Higher particle size was observed for

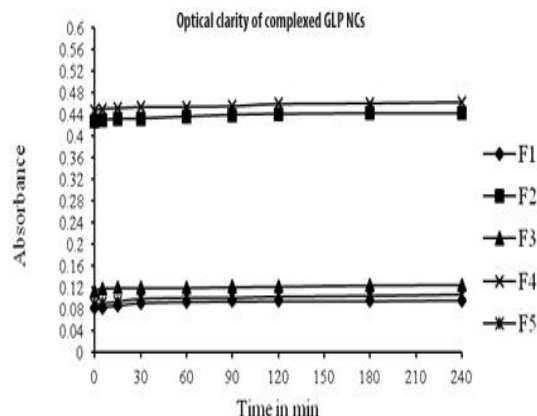


**Figure 1.** Optical clarity plot of complexed GLP NCs.

precipitated NCs (formulations F1 to F5), may be due to instability or aggregation. The mean particle size of complexed NCs was between 210 to 550 nm. Amongst the complexed formulations, the formulation

with drug to polymer ratio of 1:1, F1P exhibited the lowest particle size of 240 nm.

The PDI of complexed NCs was higher in comparison to pure GLP (0.252) and

precipitated NCs, indicating that the particles were highly polydisperse in nature.

**Table 2.** Particle size, Poly dispersity index and zeta potential data of precipitated and complexed GLP NCs

| PEG NCs (precipitated) |              |              |              | P90G NCs (complexed) |              |              |              |
|------------------------|--------------|--------------|--------------|----------------------|--------------|--------------|--------------|
| Batch                  | Z.avg (d.nm) | PDI (avg.)   | Avg. ZP (mV) | Batch                | Z.avg (d.nm) | PDI (avg.)   | Avg. ZP (mV) |
| Pure GLP               | 2066 ± 0.35  | 0.252 ± 0.25 | -40.2 ± 0.01 | -                    | -            | -            | -            |
| F1                     | 1650 ± 0.01  | 0.367 ± 0.13 | -40.7 ± 0.01 | F1P                  | 240 ± 0.02   | 0.766 ± 0.15 | -59.0 ± 0.05 |
| F2                     | 1920 ± 0.04  | 0.460 ± 0.01 | -42.1 ± 0.12 | F2P                  | 550 ± 0.16   | 0.604 ± 0.04 | -54.4 ± 0.03 |
| F3                     | 1593 ± 0.13  | 0.673 ± 0.04 | -41.4 ± 0.04 | F3P                  | 281 ± 0.05   | 1.0 ± 0.07   | -51.7 ± 0.16 |
| F4                     | 307 ± 0.25   | 0.743 ± 0.06 | -39.1 ± 0.21 | F4P                  | 210 ± 0.03   | 0.847 ± 0.18 | -51.5 ± 0.21 |
| F5                     | 30 ± 0.04    | 0.212 ± 0.32 | -31.6 ± 0.47 | F5P                  | 249 ± 0.18   | 1.0 ± 0.06   | -41.7 ± 0.04 |

± indicates SD (n=3)

#### 9.4 Zeta Potential

The average ZP of pure GLP, precipitated and complexed NCs were compared in Table 2. A ZP of -40.2 (mV) was observed for pure GLP. Higher ZP was observed in all complexed NCs indicating an increase in stability.

#### 9.5 X-Ray Powder Diffraction

The diffraction spectra of pure GLP, PM (1:1) and complexed NCs are illustrated in Fig.2A and 2B respectively. Numerous sharp and narrow intense peaks were observed at 17.82°, 20.77°, 21.06°, 22.69°, 26.02° and 53.82° in pure GLP spectra proving its high crystallinity. The XRPD spectra of physical mixture (GLP: PEG-1:1) showed less intense peaks with decrease in peak area. Numerous, less intense, slightly broadened peaks with reduced sharpness and low peak area were observed in the spectra of all NCs. These spectral changes may owe to the changes in crystal size of samples.

#### 9.6 Differential Scanning Calorimetry

DSC thermograms of GLP, PEG 20000, PM (1:1) and complexed NCs are compared in Fig.3A and Fig.3B respectively. A sharp endothermic peak at 213.8°C ( $\Delta H = 43.1$  J/g) in pure GLP thermogram indicated its high crystallinity. An endothermic peak at 65.24°C in PEG 20000 thermogram reveals its crystalline nature ( $\Delta H = 187.6$  J/g). A single endothermic peak at 69.9°C ( $\Delta H = 71.0$  J/g) was observed in the thermogram of physical mixture (1:1), due to the fusion of the components and thus indicates some modifications due to the presence of PEG 20000.

The endothermic peak values of all complexed NCs were between 167.0-167.7°C and exhibited a decrease in peak values as compared to pure GLP. The  $\Delta H$  (J/g) of NCs was also found to vary within the batches.

#### 9.7 FT-IR Analysis

FT-IR spectra of pure GLP, PEG 20000, PM (1:1) and precipitated NCs were

compared in Fig.4A and Fig.4B respectively. Pure GLP exhibited characteristic bands at  $3366\text{ cm}^{-1}$  and  $2946\text{ cm}^{-1}$  (NH and C-H aromatic stretching),  $1683\text{ cm}^{-1}$  (C=O stretching),  $1532\text{ cm}^{-1}$  and  $1443\text{ cm}^{-1}$  (N=O stretching),  $1345\text{ cm}^{-1}$  (C-N

stretching) and  $1153\text{ cm}^{-1}$  (S=O stretching) respectively (Hindustan et al., 2005). The presence of characteristic peaks of GLP in all NCs proved the absence of interaction between drug and the polymer.

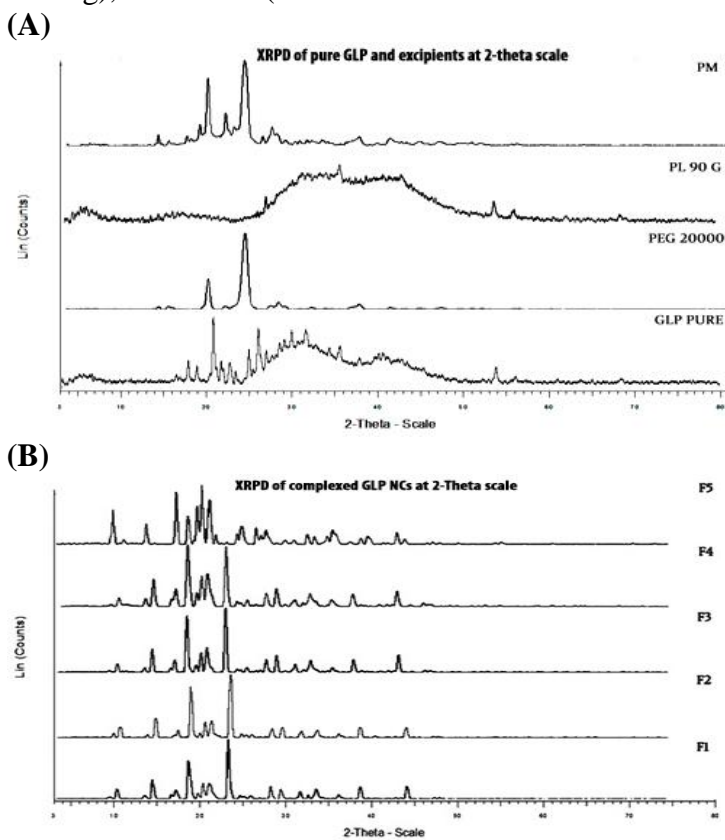


**Figure 2.** XRPD of pure GLP, PEG 20000, P90G and PM (1:1) (A), and complexed GLP NCs, (F1-F5) at 2-Theta-scale (B).

### 9.8 Surface Morphology Analysis

The SEM images of pure GLP (Fig.5A) showed numerous irregularly shaped particles of large size ( $> 5\mu\text{m}$ ). The precipitated NCs were polyhedron in shape, and were aggregated before complexation (Fig.5B). Surface morphology of complexed NCs exhibited numerous, uniform, spherically shaped particles of size below  $1000\text{ nm}$ , possessing a lipid coat on the surface. (Fig.5C). Fig.5D shows images of air drying. Fig.5E shows aggregated NCs before complexation and after microscopical examination. These observations reveal a

distinct difference in surface morphology of pure GLP and complexed NCs.

### 9.9 In Vitro Dissolution Studies

The dissolution profiles of pure GLP and complexed GLP-PEG NCs are illustrated in Fig.6. A higher cumulative percentage release (CPR) was observed in NCs than pure GLP. The dissolution profile of all the formulations were quite similar, whereas the formulation F1P exhibited a cumulative percentage release of  $98.42\%$  at the end of 4h, while pure GLP attained only

28.82%. Based on these observations formulation F1P was found to be the most satisfactory formulation. The quantity of drug released at specified time ( $Q_{min}$ ) interval from all the complexed GLP-PEG NCs formulations was compared with each

other, as well as with the pure GLP. The amount of drug released at different time intervals ( $Q_{5min}$ ,  $Q_{10min}$ ,  $Q_{30min}$  and  $Q_{60min}$ ) was higher in all formulations compared to pure GLP.

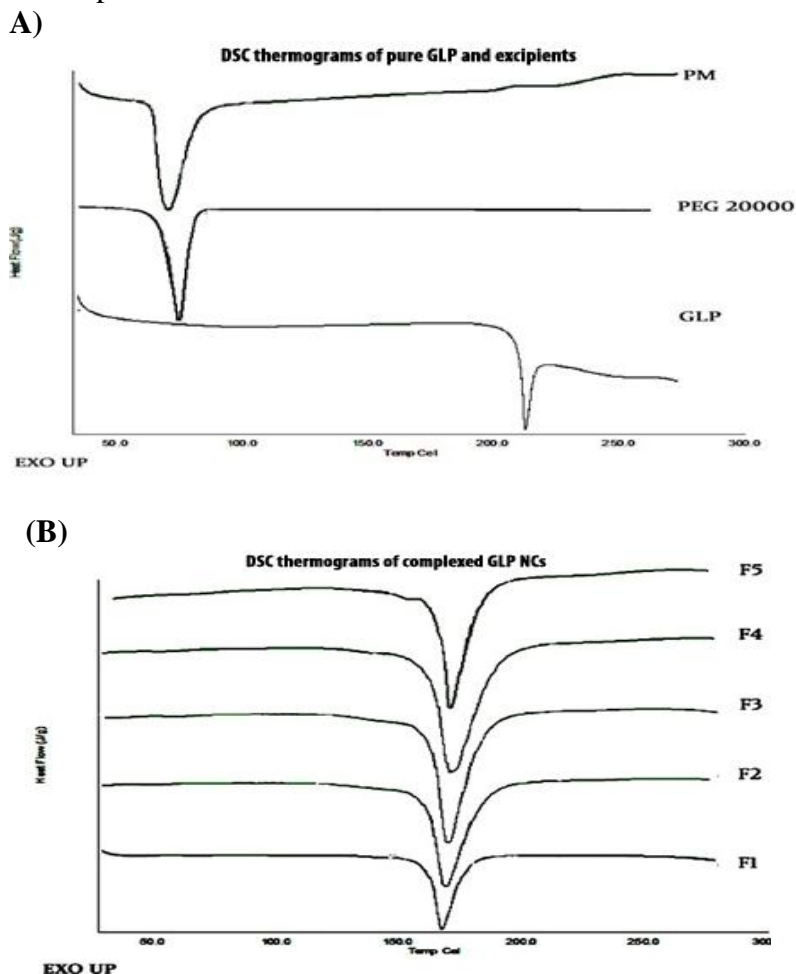


**Figure 3.** DSC thermograms of pure GLP, PEG 20000 and PM -1:1 (A), and complexed GLP NCs F1-F5 (B).

The dissolution efficiency of complexed formulations at the 60<sup>th</sup> min was in the order of F1P > F4P > F5P > F2P > F3P > pure GLP. On the contrary, the mean dissolution time of the most satisfactory formulation F1P was the minimum.

### 9.10 In-Vivo Studies

The in-vivo studies carried out on male Wistar rats indicated, better concentration of GLP in rat pancreas, with the most satisfactory formulation F1P compared to pure GLP. Also it was observed that the GLP concentration in pancreas, from the control (GLP-PEG NCs – formulation F1) was almost same as that of pure GLP (Table 3). The drug concentration (test sample -1P) in pancreas was 1.38  $\mu\text{g/ml}$ ,

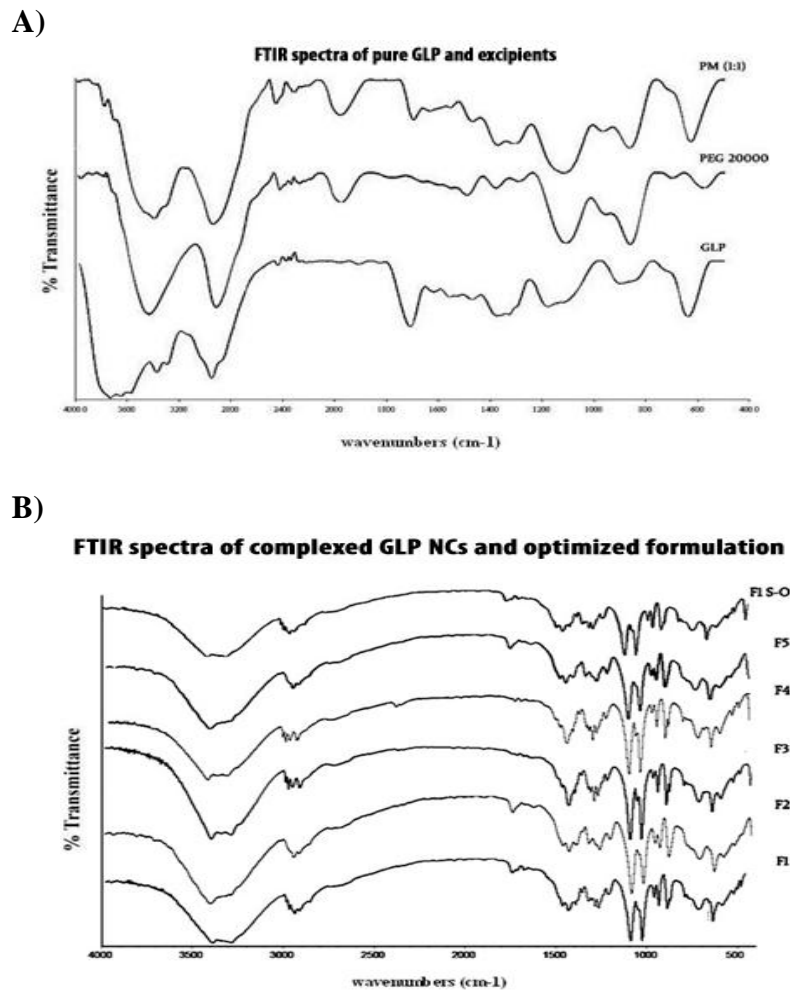


**Figure 4.** FTIR spectra of pure GLP, PEG 20000 and PM -1:1 (A), precipitated GLP NCs (F1-F5) and optimized formulation (F1-S-O) after 3 months of storage (B).

whereas those of pure GLP and precipitated NC were 1.36  $\mu\text{g/ml}$  respectively after 1 h. The HPLC chromatograph of pure GLP, test sample (F1P) and precipitated NCs (F1) showed RT of 3.4 min. There was no endogenous peak in the chromatograms interfering with GLP or with the internal standard (0.1% Orthophosphoric acid). The GLP peaks were well separated from the internal standard without any interference. The concentration of GLP in pancreas, obtained from pure GLP, complexed GLP-PEG NCs and GLP-PEG NCs was further subjected for one-way ANOVA test,

students't' test and post hoc Bonferroni test. The difference was found to be significant ( $p < 0.001$ ).

### 9.11 Short Term Stability Studies

The stability data of most satisfactory formulation (F1P) is given in Table 4. No significant changes in drug content and particle size were observed during the storage period. The drug content and average particle size were found to be 42% and 240 nm respectively. The FT-IR spectra of most satisfactory formulation (F1P)

(Fig.5B) was found to possess all the major characteristic peaks of pure GLP.

## 10. DISCUSSION

Lipid NCs (LNCs) are complexed NCs containing drug, polymer and lipid (phospholipids), designed to alter the pharmacokinetics of glimepiride. This may have higher bioavailability, *in vivo* stability

and perhaps help in better drug targeting. PEG 20000 was polymer of choice for Nanonization as it is nontoxic, applicable to drug carriers and widely used in solubility enhancement studies. Also, PEG exhibited higher particle size reduction ensuring higher saturation solubility [41].

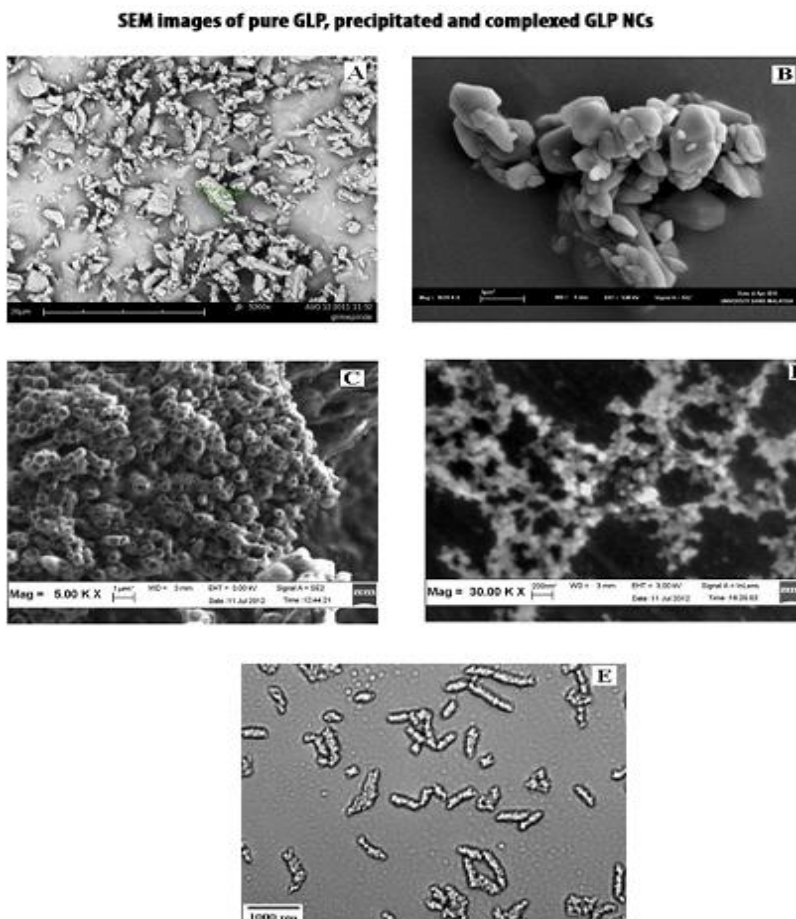


**Figure 5.** SEM images of pure GLP (a), precipitated F1 NCs (b), complexed FIP NCs (c), FIP NCs dispersed in water and air dried (d) and precipitated NCs in aggregated form before complexation (e).

In the study initially GLP-PEG NCs were prepared by controlled precipitation in presence of surfactants. Though these formulations effectively improved solubility they were exhibiting poor surface properties. Stability was a concern with GLP-PEG NCs, as they continuously formed aggregates, on

exposure to medium, leading to increased particle size. Such stability issues may affect drug delivery or targeting, causing a decline in, *in vivo* performance of the drug. This issue was dealt by addition of Tween 80 (2.5%w/v) during the process of milling, resulting in less particle aggregation.

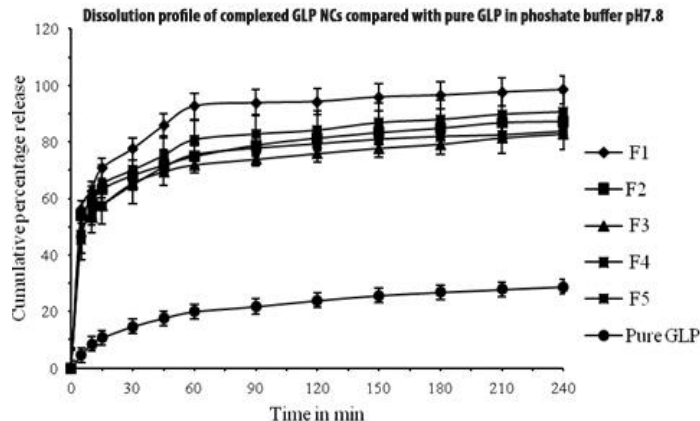


**Figure 6.** Dissolution profiles of complexed GLP NCs in phosphate buffer pH 7.8 compared with pure GLP. All data points represent the mean value.

**Table 3.** Retention time (RT), peak area and concentration of pure GLP in comparison with test formulations.

| Batch                 | Retention Time (RT) | Peak Area (AUC) 1 h | Conc. in pancreatic tissue ( $\mu\text{g/ml}$ ) |
|-----------------------|---------------------|---------------------|---|
| Pure GLP              | $3.4 \pm 0.03$      | $86059 \pm 1105$    | $1.36 \pm 0.11$                                 |
| Precipitated NCs (F1) | $3.4 \pm 0.02$      | $84731 \pm 1002$    | $1.36 \pm 0.32$                                 |
| Test Sample (F1P)     | $3.4 \pm 0.08$      | $138027 \pm 1043$   | $1.38 \pm 0.45$                                 |
| *P value -t- test     | * $p > 0.05$        | * $p < 0.001$       | * $p < 0.001$                                   |

$p \leq 0.05$ , Statistical significant test was done by one way ANOVA followed by students 't' test.  $\pm$  indicates SD ( $n=3$ )

**Table 4.** Stability data of optimized complexed NC (F1P)

| Stability conditions | Parameters       | Observation (months) |                  |                   |                   |
|----------------------|------------------|----------------------|------------------|-------------------|-------------------|
|                      |                  | 0                    | 1                | 2                 | 3                 |
| Room Temperature     | Drug content (%) | $42.30 \pm 1.48$     | $42.21 \pm 0.85$ | $41.90 \pm 0.94$  | $41.90 \pm 1.27$  |
|                      | Z.avg (d.nm)     | $240.4 \pm 0.027$    | $240.1 \pm 0.73$ | $241.5 \pm 0.085$ | $241.7 \pm 0.161$ |
| 40°C (RH 75%)        | Drug content (%) | $42.05 \pm 1.02$     | $41.85 \pm 0.34$ | $41.73 \pm 1.13$  | $41.71 \pm 0.76$  |
|                      | Z.avg (d.nm)     | $240.4 \pm 0.019$    | $240.8 \pm 0.17$ | $241.5 \pm 0.179$ | $242.7 \pm 0.158$ |

$\pm$  indicates SD ( $n=3$ )

Therefore, *in vitro* and *in vivo* stability considerations of nanoparticulates are challenging and should be given prime

importance during development of formulations.

Development of stable NCs (both *in vitro* and *in vivo*) with targeting features is quite

troublesome. Also, a drug which is stable *in vitro* can exhibit different pharmacological response *in vivo* or while in contact with body fluids. This may ultimately decrease the pharmacokinetic profile of the drug. *In vivo* stability is vital for nano-formulations as it displays the consistent behaviour of drugs as well as their efficiency in drug delivery. The limitations occurring in precipitated NCs could be resolved by complexation approach [42].

Recently, lipids (soybean lecithin) and phospholipids (P90G) are widely explored to develop nanoparticulates and to improve the stability and targetability of drugs. In a suitable study, soybean lecithin improved the *in vitro* stability of glibenclamide, but exhibited decreased *in vivo* performances, hence lowering the targeting efficiency [43]. Decreased targetability may be as a result of high complexity, low lipophilicity and presence of impurities in lipids [44]. Selection of appropriate lipid for stability enhancement, perhaps improves better drug distribution through reduced particle aggregation. These include considerations like composition, lipophilicity, compatibility and solubility of lipid with the drug. Consequently, in this study, to enhance the surface properties of precipitated GLP-PEG NCs, these were complexed with a lipid (phospholipon 90G). By formulating GLP-PEG NCs and further complexing these NCs with lipids, may improve the surface properties. This will probably help in targeting GLP to pancreas and facilitate higher insulin secretion.

In the present study, P90G was chosen as complexing agent owing to its high purity, emulsifying and stabilizing properties [45]. P90G is purified phosphatidylcholine from soybean lecithin. These phospholipids can spontaneously form spherical shaped membranes which encloses an aqueous volume to form liposomes in an aqueous environment [46].

Complexation of NCs using phospholipids (P90G) forms a steric barrier between the NCs and the dispersion medium, reduces aggregation and increases the stability [47]. To attain complexation, GLP was first solubilized in DCM and to this mixture PEG was added, followed by addition of phospholipon by continuous stirring as discussed in above procedure. GLP form complex with PEG by hydrogen bonding interactions between the electro negative carbonyl groups of phospholipon and nitrogen groups of GLP, with polar groups of PEG. This complex upon addition onto water having Tween80 triggers the rapid crystallization of GLP. The process was evident by DSC and XRD studies with change in melting temperature and crystallinity.

The mechanism of complexation involves heating and subsequent cooling of dispersion. Expansion of organic phase occurred, when the mixture of chloroformic solution of P90G and GLP-PEG NCs was heated below the melting point of P90G (60°C). During this step NCs moved outside from the core. On subsequent cooling (cold melt), the NCs entered into the core of the system. Further, on cooling (15°C for 1 h) the lipids were physically adsorbed on to the surface of NCs (GLP-PEG-P90G) forming spherically shaped particles. The complexed GLP-PEG NCs thus obtained were subjected for various evaluation parameters.

The DL efficiency was found to increase with higher PEG concentration (Table 1). Also, the saturation solubility of P90G NCs was found to increase by three folds resulting in improved drug solubility. The SS was found to increase in NCs due to the creation of high energy surfaces when microparticles were disrupted into nanoparticles. High SS could be related to exposure of lyophilic inner surfaces of the particles to the aqueous dispersion medium. These results were in accordance with the

report of solubility studies conducted on various BCS class II drugs using PEG 20000 [48].

Lipids used in the formulation also aids in solubility of the drug. This involves selection of suitable surfactant with low HLB (tween 80). In this case the drug should be first dissolved into lipid, followed by heating above its melting point. Also the solubility of drug is aided by the concentration of lipid and surfactant added.

Drug delivery depends on the type of NPs, particle size, surface properties and stability of the particles in the medium [49]. In our study, it was crucial that the processed NCs remain as fine dispersions. To evaluate the property, optical clarity measurements were performed. Visual appearance and clarity were also observed for the presence of any particular matter. A low absorbance value is expected for clear solution, whereas higher absorbance values were likely for cloudy solution [50]. Cloudy solutions scatter more of incident radiation, viewing higher absorbance and hence high crystallinity [51]. In our examination, batch F1P was found to be less cloudy and possessed higher clarity (Fig.1).

In particle characterization reports, the average particle size and PDI of NCs were found to vary with respect to its polymer concentration. A high particle size was observed for precipitated NCs due to high proportion of PEG in NCs that led to an increase in particle size due to plasticization resulting in instability and formation of agglomerates [52]. Based on these findings, formulation F1P was found to be the most satisfactory, with minimal particle size. A high ZP was observed in all complexed NCs indicating an increase in stability as compared to pure GLP (Table 2). The increased stability of complexed NCs may be attributed to the repulsive force associated with it and a reduction in particle agglomeration due to the presence of P90G.

XRPD results showed that relative intensity values (d-value) decreased initially and became constant at later stages proving that the complexed formulations still exist as crystals. A shift in diffraction pattern was noticed in NCs which indicated a change in crystal size due to the presence of PEG (Fig.3B). The above results showed that crystallinity of GLP was not altered in presence of PEG and P90G. The absence of interaction between drug and polymer was also observed with LNCs exhibiting similar characteristic diffraction patterns as that of GLP, at 20.77°, 24.91° and 26.02° 2 $\theta$  positions.

In DSC analysis, a shift in melting peak to a lower temperature was observed in all LNCs. This could be ascribed to some structural changes that would have occurred during the process of complexation and lyophilisation [53]. The presence of low crystallinity in optimized sample (F1) was evident from the absence of endothermic peak at 213.8°C ( $\Delta H = 43.1$  J/g) (Fig.4B). These complexed NCs may provide higher solubility and stability than pure GLP. The variation in  $\Delta H$  (J/g) of NCs amongst formulations clearly proves that crystallinity was maintained in all NCs but with slight degree of disorientation in their crystal structures.

The morphological evaluation by SEM revealed a distinct difference in surface morphology of pure GLP and complexed NCs. Higher dissolution rates are achieved by reduction in particle size. Smaller particles have larger surface area and thus exhibit higher saturation solubility. In this study the NCs obtained from precipitation with smaller particles tend to get into solution form faster and produce a higher release (>61%) upon contact with medium. Complexed LNCs exhibited an initial release of 56% within 5 min, compared to pure GLP (5%) and then the drug release was constant up to 240 min (Fig.2). Slow

drug dissolution may be due to P90G coating, higher polymeric concentration and higher diffusional path length. It was observed that drug dissolution from LNCs never reached completion. This may owe to linear nature of polymer and unknown complex formation [54].

Phosphate buffer (pH 7.8) was selected for the study as it was highly relevant to the physiological conditions of drug dissolution sites in the body and also justified on case by case basis as per FIP guidelines, as it should not exceed pH 8. A pH of 7.8 also showed a significant rate of absorbance in the UV range (1  $\mu\text{g}/\text{ml}$ ) [55]. MDT (60 min) and % DE (60 min) were calculated to study the effectiveness of drug dissolution. All the batches experienced a lower MDT and a higher % DE in comparison to pure GLP. The MDT of batch F1P (13.90 min) was found to be less, due to effective particle size reduction. The amount of drug released (mg) from complexed GLP NCs at different time interval ( $Q_{5\text{min}} - Q_{60\text{min}}$ ) was found to be higher ( $> 0.18$ ) in all batches compared to pure GLP. A higher drug release of 3.70 mg was observed for F1P formulation, while in pure GLP it was only 0.79 mg at 60 min.

The dissolution efficiency of batch F1P was higher compared to all batches. The order of percentage dissolution efficiency at 60 min can be expressed as F1P (88.74)  $>$  F4P (76.50)  $>$  F5P (71.25)  $>$  F2P (70.75)  $>$  F3P (67.39)  $>$  pure GLP (18.57). The data was found to be in accordance to dissolution studies. Batch F1P experienced less time to get into solution faster compared to other batches and pure GLP. These findings also correlate with the *in vitro* results and based on these interpretations it can be suggested that batch F1P was most ideal batch in the lot.

P90G complexation was aimed to improve the *in vitro* and *in vivo* stability of GLP. In addition, it was intended to enhance the

biological performance of the drug. GLP is distinct from other sulfonylureas as it is incorporated into the 65-kDa protein binding site on  $\beta$ -cells. Considering the mechanism of action of GLP, it is likely to bind to ATP-sensitive K<sup>-</sup> channel receptors on the pancreatic cell surface, inducing secretion of insulin. Higher binding efficiency of LNCs may offer therapeutic success.

*In vivo* studies on optimized LNCs reveal an equivalent amount of drug (1.38 $\mu\text{g}/\text{ml}$ ) in pancreas of rat as that of GLP and precipitated NCs after 1 h (Table 4). The AUC was found to be higher in optimized samples (F1P). A higher AUC indicate improved bio-distribution and higher *in vivo* stability. This may be correlated to decreased particle size (Z.avg, 240nm) (Fig.6D) and higher circulation of NCs in blood owing to complexation [56]. The AUC of precipitated NCs (F1) was less, indicating decreased uptake of drug by pancreas. An equivalent drug distribution from LNCs was unpredictable and it may be due to wider distribution of particles (0.766). The factors responsible for variation in drug distribution include lipophilicity of P90G to gut wall and the role of enterocytes and M-cells in the oral absorption of NCs [57-59]. Few studies have demonstrated that the nature of phospholipids and density of coating might influence higher AUC and binding of drugs to pancreatic tissues [60]. P90G favours higher AUC and improved *in vivo* stability due to high phosphatidylcholine content (94.0 -102%), and suitable amphiphilic character.

Short term stability studies carried out for the F1P formulation indicated that the formulation was stable. The FT-IR spectra of the most satisfactory formulation (F1P) were found to have all the major characteristic peaks of pure GLP. This clearly proves that the chemical identity of GLP was preserved in the samples. All the

above findings reveal that the formulation was stable.

## 11. CONCLUSIONS

To conclude, the study provides an outlook into the possible consideration to be made in the development of stable nanoparticles for drug delivery. GLP NCs were formulated by precipitation process and complexed using phospholipids in sequence to improve the solubility, stability and targeting efficiency of the drug. The formulation parameters that influenced the formation of drug NCs were investigated and optimized. The increase in saturation solubility three times, superior dissolution and *in vitro* stability of NCs compared to pure GLP could be linked to effective size reduction and complexation. In - process characterization studies showed no drug - excipient interactions or change in drug properties.

*In vivo* studies on optimized NCs exhibited slightly better drug concentration in pancreas compared to that of pure GLP during 1 h. It could be concluded that PEG 20000 and P90G are effective polymer and stabilizer for solubility and stability enhancement of nanoparticulates. P90G complexation may evade *in vitro* and *in vivo* stability issues of nanoparticulates and aid in development of firm nanocrystals. This approach might improve the overall pharmacokinetics of the glimepiride.

## COMPETING INTERESTS

The authors report no conflicts of interest.

## ACKNOWLEDGEMENTS

The authors would like to thank Acharya and BM Reddy College of Pharmacy, Bengaluru, India, AIMST University and Universiti Sains Malaysia (USM), Malaysia, and SAIF-STIC, Cochin, India for their laboratory and instrumentation analysis support.

## REFERENCES

1. Shaik, R., Bilal, A. T., (2012). "Nanomedicine current trends in diabetes management", *J. Nanomed. Nanotech.*, 3: 1-7.
2. Gangadhara, A. R., Subashini., (2014). "Transdermal Nanocarriers: New Challenges and Prospectives in the Treatment of Diabetes mellitus", *J. of Chem. and App. Biochem.*, 1: 1-11.
3. Silvio, E., Inzucchi., (2015). "Management of hyperglycemia in Type 2 diabetes. A patient centered approach", *Diabetes Care.*, 38: 140-149.
4. Sajeev, K. B., Saraswathi, R., (2013). "Development and characterization of lecithin stabilized glibenclamide nanocrystals for enhanced solubility and drug delivery", *Drug Delivery.*, 21: 173-184.
5. Williams, R. O., (2012). "*Preface in formulating poorly water-soluble drugs*", Springer, USA.
6. Thomas, T., Jennifer, B., (2012). "New formulation approaches to improve solubility and drug release from fixed dose combinations: case examples, Pioglitazone / glimepiride and ezetimibe / simvastatin", *Eur. J. Pharm. Biopharm.*, 84: 208-18.
7. Gülsun, T., Gürsoy, R. N., (2009). "Öner. Nanocrystal technology for oral delivery of poorly water soluble drugs", *J. Pharm. Sci.*, 34: 55-65.
8. Chen, H., Khemtong, C., Yang, X., (2011). "Nanonization strategies for poorly water soluble drugs", *Drug Discov. Today.*, 16: 354-60.
9. Faris, N. B., Müller, R. H., (2002). "Nanocrystals for poorly soluble drugs for oral administration", *New Drugs.*, 2: 20-21.
10. Melike, Ü., Gülgün, Y., (2007). "Importance of solid lipid nanoparticles (SLN) in various administration routes and future perspectives", *Int. J. Nanomed.*, 2: 289-300.
11. Mishra, B., Bhavesh, P., (2010). "Colloidal nanocarriers- a review on formulation technology, types and applications towards targeted drug delivery", *Nanomed, Nanotechnol. Biomed.*, 6: 9-24.
12. Fillipos, K., Santipharp, P., (2007). "Nanosizing oral formulation development and biopharmaceutical evaluation". *Adv. Drug Deliver. Rev.*, 59: 631-644.

13. Faris, N. B., Rainer, R. H., (2002). "Nanocrystals technology drug delivery and clinical applications". *Int. J. of Nanomed.*, 3: 295-309.
14. Mohanraj, V. J., Chen, Y.,(2006). "Nanoparticles - A Review", *Trop. J. Pharm. Res.*, 5: 561-573.
15. Sandrine, D., Lucie, S., (2012). "Physico-chemical parameters that govern nanoparticles fate also dictate rules for their molecular evolution", *Adv. Drug Deliver. Rev.*, 64: 179-189.
16. Zheng, N., Gao, X., Song, Q., (2012). "Lipid - based liquid crystalline nanoparticles as oral drug delivery vehicles for poorly water - soluble drugs, cellular interaction and in vivo absorption", *Int. J. Nano. Med.*, 7: 3703-3718.
17. Huabing, C., Chalermachai, K., (2011). "Nanonization strategies for poorly water soluble drugs", *Drug Discov. Today.*, 16: 354-360.
18. Libo, W., Jian, Z., (2011). "Physical stability of nanoparticles", *Adv. Drug Deliver. Rev.*, 63: 456-469.
19. Frick, A., Moller, H., Wirbitzki, E., (1998). "Biopharmaceutical characterization of oral immediate release drug products. *Invitro/invivo* comparison of phenoxymethyl pencillin, glimepiridie and levofloxacin". *Eur. J. of Pharm. Biopharm.*, 46: 305-311.
20. Hai, W., Chad, D., (2008). "Physiochemical characterization of five glyburide powders. A BCS based approach to predict oral absorption". *Eur. J. of Pharm. Biopharm.*, 46: 305-311.
21. Patrick, J. C., Luigi, G. M., (2004). "Formulation design: new drugs from old. *Drug discov. today, therap. and strategies.*, 1: 537-542.
22. O'Donnell, K. P., (2012). "*Optimizing the formulation of poorly water - soluble drugs*". Springer, USA.
23. Otilia, M. K., (2005). "Role of nanotechnology in targeted drug delivery and imaging: a concise review", *Nanomed. Nanotechol. Biomed.*, 1: 193-212.
24. Melgardt, M. D., (2009). "*Nanotechnology in drug delivery*". AAPS Press, USA.
25. Mishra, B., Bhavesh, P., (2010). "Colloidal nanocarriers: A review on formulation technology, types and applications towards targeted drug delivery", *Nanomed. Nanotechol. Biomed.*, 6: 9-24.
26. Shelesh, J., Swarnalata, S., (2010). "Type 2 Diabetes Mellitus - Its global prevalence and therapeutic strategies", *Diabetes Metab. Syndrome Clin. Res. Rev.*, 4: 48-56.
27. Mihaela, M. M., Helen, L. M., (2011). Glimepiride, a novel sulfonylurea does not abolish myocardial protection afforded by either ischemic preconditioning or diazoxide, *J. American Heart Association.*, 103: 3111-3116.
28. Rhoban, T., (2005). "The efficacy and safety of glimepiride in the management of Type II diabetes in Muslim patients during Ramadan", *Diabetes Care.*, 28: 421-422.
29. Vania B. B., (2010). "Preparation of PVP hyrogel nanoparticles using lecithin vesicles", *Quim. Nova.*, 33: 2083-2087.
30. Tongying, J., Ning, H. (2012). "Enhanced dissolution rate and oral bioavailability of simvastatin nanocrystals prepared by sonoprecipitation", *Drug Dev. Ind. Pharm.*, 38: 1230-1239.
31. Afe, H., Göpferich, A., (2008). "Polymer coating of quantum dots - a powerful tool towards diagnostics and sensorics", *Eur. J. Pharm. Biopharm.*, 68: 138-152.
32. Sohelia, K., Abbas, H. A., (2011) "New surface-modified solid lipid nanoparticles using N-glutaryl phosphatidylethanolamine as the outer shell", *Int. J. Nanomed.*, 6: 2393-2401.
33. Baliar, S., Biswal, S., (2009). "Physiochemical properties of glimepiride in solid dispersions with polyethylene glycol 20000", *Int. J. Pharm. Sci. Nano.*, 2: 537-543.
34. Blagden, N., Maras, M., (2007). "Crystal engineering of active pharmaceutical ingredients to improve solubility and dissolution rates", *Adv. Drug Deliver. Rev.*, 59: 617-630.
35. Fuminori, I., Hiroyuki, F., (2008). "Effect of polyethylene glycol on preparation of rifampicin-loaded PLGA microspheres with membrane emulsification technique", *Colloids Surf. B: Biointerfaces.*, 66: 65-70.
36. Min, S. K., Shun, J. J., (2008). "Preparation, characterization and *in vivo* evaluation of amorphous atrovastatin calcium nanoparticles using supercritical antisolvent (SAS) process", *Eur. J. Pharm. Biopharm.*, 69: 454-465.
37. Hui, S. W., Kuhl, T. L., (1999). "Use of polyethylene glycol to control cell aggregation and fusion". *Colloids Surf. B: Biointerfaces.*, 4, 213-222.
38. Shubhadeep, C., Subhabrota, M., (2010). "Statistical optimization of fixed dose combination of glimepiride and atrovastatin calcium in immediate release tablet formulation", *Int. J. Pharm. Sci.*, 2: 194-200.
39. Korsmeyer, R. W., Gurny, R., (1983). "Mechanism of solute release from porous hydrophilic polymers", *Int. J. Pharm.*, 15: 25-35.
40. Kim, H., Fassih, R., (1997). "Application of binary polymer system in drug release rate modulation and influence of formulation variables and hydrodynamic conditions on release kinetics", *J. Pharm. Sci.*, 86: 323-328.

41. Hörter, D., Dressman, J. B., (1997). "Influence of physiochemical properties on dissolution of drugs in the gastrointestinal tract", *Adv. Drug Deliver. Rev.*, 25: 3-14.
42. Kaili, H., Shan, C., (2012). "Enhanced oral bioavailability of doxorubicin by lecithin nanoparticles: Preparation, in vitro and in vivo evaluation". *Int. J. Nano. Med.*, 7: 3537-3545
43. Zhipeng, C., Lu, X., (2012). "Novel materials which possess the ability to target liver cells". *Drug Delivery.*, 9: 649-656.
44. Sajeev, K. B., Saraswathi, R., (2011). "Formulation and evaluation of controlled release glimepiride osmotic systems", *Int. J. Pharm. Res.*, 3: 79-84.
45. Kaili, H., Shan, C., (2012). "Enhanced oral bioavailability of doxorubicin by lecithin nanoparticles: Preparation, in vitro and in vivo evaluation", *Int. J. Nano. Med.* 7: 3537-3545.
46. Brown, N. J., Read, N. W., (1990). "Characteristics of lipid substance activating the ideal break in the rat", *Gut.*, 31: 1126-1129.
47. Jane, W., Sabine, G., (2008). "Physicochemical stability of phospholipid-dispersed suspensions of crystalline itraconazole", *Eur. J. Pharm. Biopharm.*, 69: 1104-1113.
48. Robash, K. S., Keon, W. K. (2009). "Preparation and characterization of solid lipid nanoparticles loaded with doxorubicin", *Eur. J. Pharm. Sci.*, 37: 508-513.
49. Müller, R. H., Jacobs, C., Kayser, O., (2001). "Nanosuspensions as particulate drug formulations in therapy, rationale for development and what we can expect for the future", *Adv. Drug Deliver. Rev.*, 47: 3-19.
50. Fuminori, I., Hiroyuki, F., (2008). "Effect of polyethylene glycol on preparation of rifampicin-loaded PLGA microspheres with membrane emulsification technique". *Colloids. Surf. B. Biointerfaces.*, 66: 65-70.
51. Avnesh, K., Sudesh, K. Y., (2010). "Biodegradable polymeric nanoparticles based drug delivery systems", *Colloids Surf. B. Biointerfaces.*, 75: 1-18.
52. Marie, G., Angelica, V., (2008). "Nanoparticles for drug delivery: The need for precision in reporting particle size parameters". *Eur. J. Pharm. Biopharm.*, 69: 1-9.
53. Shasha, R., Yunmei, S., (2012). "Particle size reductions to the nanometer range a promising approach to improve buccal absorption of poorly water-soluble drugs", *Int. J. Nano. Med.*, 6: 1245-1251.
54. Tamara, M. (2005). "Soluble polymer conjugates for drug delivery", *Drug Discov. Today Tech.*, 2: 15-20.
55. Anju, G., Singhvi, I., (2007). "Simultaneous spectrophotometric estimation of Rosiglitazone maleate and glimepiride in tablet dosage forms", *Indian J. Pharm. Sci.*, 69: 780-783.
56. Lisha, W., Yanxia, J., Wei, G., (2015). "Preparation, physical characterization and pharmacokinetic study of paclitaxel nanocrystals", *Drug. Dev. Ind. Pharm.*, 41: 1343-1352.
57. Yue, P. F., Yuan, H. L., (2010). "Process, optimization, characterization and evaluation in vivo of oxymatrine-phospholipid complex", *Int. J. Pharm.*, 387: 139-146.
58. Yongxue, Z., Chunling, W., (2012). "A frustrating problem, accelerated blood clearance of PEGylated solid nanoparticles following subcutaneous injection in rats", *Eur. J. Pharm. Biopharm.*, 81: 506-513.
59. Fu, Q., Sun, J., Zhang, D., "Nimodipine nanocrystals for oral bioavailability improvement: preparation, characterization and pharmacokinetic studies", *Colloids Surf. B. Biointerfaces.*, 109: 161-166.
60. Tony, R., Elisabeth., (1991). "Determination of glibenclamide and its major metabolites in human serum and urine by column liquid chromatography", *J. Chrom.*, 564: 223-233.